CrystEngComm

View Online / Journal Homepage
Dynamic Article Links

Cite this: DOI: 10.1039/c2ce25898f

www.rsc.org/crystengcomm

PAPER

Influence of ligand substituent on structural assembly and coordination geometry†

Hamid Reza Khavasi,* Maryam Mehdizadeh Barforoush‡ and Mahmood Azizpoor Fard‡

Received 5th June 2012, Accepted 6th August 2012
DOI: 10.1039/c2ce25898f

In this study, *N*-(aryl)-2-pyrazinecarboxamide ligands with two different aryl groups (*o*-anisidyl, L^{OMe}, and *o*-phenitidyl, L^{OEt}, groups) have been employed for the synthesis of six Hg(II) complexes, $[HgCl_2(L^{OMe})_2]_n$, **1**, $[HgBr_2(L^{OMe})]_n$, **2**, $[HgI_2(L^{OMe})]_n$, **3**, $[Hg_3Cl_6(L^{OEt})_3{\cdot}HgCl_2(L^{OEt})]$, **4**, $[HgBr_2(L^{OEt})]$, **5**, and $[HgI_2(L^{OEt})]$, **6**, in order to get insights into the substituent effects on the molecular architecture of complexes. Structural analysis of mercury(II) halides containing L^{OMe} ligand demonstrated that the assembly process produced an infinite 1D linear chain, 1D double chain and 1D ladder chain in **1**, **2** and **3** respectively. Structural analysis showed that compounds **4–6** have non-polymeric structures. **4** resulted in a trimeric/monomeric motif while isostructural **5** and **6** compounds formed a discrete three coordinated mercury compound. Our results show that when compared to the L^{OMe} substituent, the steric properties of the L^{OEt} group significantly alter the molecular architecture and coordination sphere of complexes.

Introduction

The construction of the structures of crystalline coordination compounds[1] depends on a number of experimental variables such as the solvent,[2] time of reaction,[3] reagent ratio,[4] temperature,[5] pH,[6] guest molecules and counterions.[7] In this regard, the chemical structure of the organic ligand[8] – even the site of the substitute position – and preferred coordination geometry of the metal[9] play an important role on the formation of different molecular architecture in the complexes in the assembly processes. To make progress in controlling specific interactions in the solid state of coordination compounds, requires systematic investigations of the effects of different factors on the final structures. Despite their potential utility, there has been little attention paid to systematic studies that examine the effect of the substituent variation of the ligand on the supramolecular aggregation of coordination complexes. Controlling the supramolecular aggregation by steric groups on the ligand in several series of zinc-triad dithiolate compounds has been systematically studied by Tiekink and co-workers.[10] Recently, systematic investigation of the influence of the substituent groups of benzimidazoles on the formation of coordination frameworks of zinc and cadmium has been reported.[11] In Mondal and co-worker's paper, the role of the steric bulk and angular dispersion of the coordination site of benzene polycarboxylic acids on the crystal engineering of zinc MOFs have been shown.[12] Substituent effects on the classical[13] and non-classical hydrogen bonds and π–π[14] and C–H···π[15] interactions have also been investigated.

In the frame of a research line about π-stacking[16a] and the effect of C–H···π[16b] interaction on the crystal packing of mercury coordination compounds containing pyrazine carboxamide ligands, that the authors are developing, the effect of ligand substituent on coordination geometry and three-dimensional supramolecular architecture have been reported here. In this study, two *N*-(aryl)-2-pyrazinecarboxamide ligands carrying a different aryl groups have been employed for the synthesis of mercury(II) complexes in order to get insights into the steric effects of aryl on the structural assembly of the complexes. We selected flexible ligands, *N*-(*o*-anisidyl)-2-pyrazinecarboxamide, L^{OMe}, and *N*-(*o*-phenitidyl)-2-pyrazinecarboxamide, L^{OEt}, in which the freedom C–C and C–N single bond rotations give rise to variable conformations and the pyrazine and aryl rings can freely twist to meet the requirements of the coordination geometries of metal atoms in the assembly process. Six Hg(II) complexes of these ligands, $[HgCl_2(L^{OMe})_2]_n$, **1**, $[HgBr_2(L^{OMe})]_n$, **2**, $[HgI_2(L^{OMe})]_n$, **3**, $[Hg_3Cl_6(L^{OEt})_6{\cdot}HgCl_2(L^{OEt})_2]$, **4**, $[HgBr_2(L^{OEt})]$, **5**, and $[HgI_2(L^{OEt})]$, **6**, have been prepared by the reaction of equimolar quantities of mercury halides (chloride, bromide and iodide) in methanol solutions, Scheme 1. The structural details show that the *N*-aryl group significantly influences the structural assembly and coordination geometry of the resulting mercury(II) complexes.

Experimental section

General

All chemicals were purchased from Aldrich or Merck and used without further purification. The synthesis and recrystallization

Department of Chemistry, Shahid Beheshti University, G. C., Evin, Tehran, 1983963113, Iran. E-mail: h-khavasi@sbu.ac.ir; Fax: +98 21 22431663

† CCDC reference numbers 865862 (**1**), 865863 (**2**), 865861 (**3**), 865866 (**4**), 865865 (**5**) and 865864 (**6**). For crystallographic data in CIF or other electronic format see DOI: 10.1039/c2ce25898f

‡ These authors contributed equally.

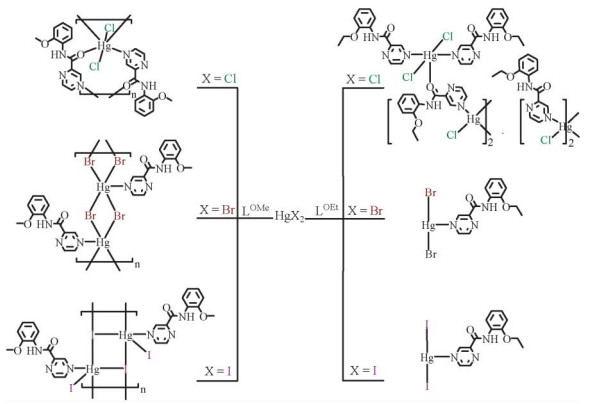

Scheme 1 Synthetic route of **1–6**.

of L^{OMe} and L^{OEt}, and compounds **1–6** were carried out in air. Infrared spectra (4000–250 cm^{-1}) of solid samples were taken as 1% dispersions in CsI pellets using a BOMEM-MB102 spectrometer. Elemental analysis was performed using a Heraeus CHN–O Rapid analyzer. ^1H NMR spectrum was recorded on a Bruker AC-300 MHz spectrometer at ambient temperature in CD_3OD. All chemical shifts are quoted in parts per million (ppm) relative to tetramethylsilane. Melting point was obtained by a Bamstead Electrothermal type 9200 melting point apparatus and corrected. Ligand *N*-(*o*-anisidyl)-2-pyrazinecarboxamide, L^{OMe}, was prepared according to the reported procedure.[17]

Single crystal diffraction studies

X-ray data for compounds **1–6** were collected on a STOE IPDS-II diffractometer with graphite monochromated Mo-Kα radiation. For $[HgCl_2(L^{OMe})_2]_n$ (**1**), a colorless needle crystal, for $[HgBr_2(L^{OMe})]_n$ (**2**), $[Hg_3Cl_6(L^{OEt})_6{\cdot}HgCl_2(L^{OEt})_2]$ (**4**), $[HgBr_2(L^{OEt})]$ (**5**), and $[HgI_2(L^{OEt})]$ (**6**), yellow block crystals and for $[HgI_2(L^{OMe})]_n$ (**3**), a yellow plate crystal was chosen using a polarizing microscope and they were mounted on a glass fiber which was used for data collection. Cell constants and an orientation matrix for data collection were obtained by least-squares refinement of the diffraction data from 3261, 4073, 4426, 14729, 4369 and 4664 unique reflections for complexes **1–6**, respectively. Data were collected at a temperature of 120(2) K for **1** and **4** and 298(2) K for **2**, **3** and **5–6** to a maximum 2θ value of 58.58°, 58.48°, 58.42°, 58.48°, 58.38° and 58.62° for **1–6**, respectively, in a series of ω scans in 1° oscillations and integrated using the Stöe X-AREA[18a] software package. A numerical absorption correction was applied using the X-RED[18b] and X-SHAPE[18c] software. The data were corrected for Lorentz and Polarizing effects. The structures were solved by direct methods[18d] and subsequent different Fourier maps and then refined on F^2 by a full-matrix least-square procedure using anisotropic displacement parameters. All hydrogen atoms were added at ideal positions and constrained to ride on their parent atoms, with $U_{iso}(H) = 1.2U_{eq}$. All refinements were performed using the X-STEP32 crystallographic software package.[18e] Crystallographic data for complexes **1–6** are listed in Table 1. Selected bond distances and angles are summarized in Table 2.

Synthesis of *N*-(*o*-phenitidyl)-2-pyrazinecarboxamide, L^{OEt}

This compound was prepared by using the previously reported method.[19]

Synthesis of mercury(II) complexes; $[HgCl_2(L^{OMe})_2]_n$, 1, $[HgBr_2(L^{OMe})]_n$, 2, $[HgI_2(L^{OMe})]_n$, 3, $[Hg_3Cl_6(L^{OEt})_6{\cdot}HgCl_2(L^{OEt})_2]$, 4, $[HgBr_2(L^{OEt})]$, 5, and $[HgI_2(L^{OEt})]$, 6

To a solution of 0.2 mmol mercury(II) halide (HgX_2, X = Cl, Br and I) in 5 mL methanol, a solution of 0.2 mmol of L in 5 mL methanol was added while stirring. The mixture was heated at 40 °C for about 30 min and then filtered. Upon slow evaporation of the filtrate at room temperature, suitable complexes for X-ray analysis were obtained after several days. It is notable that using 1 : 2 molar ratio of $HgCl_2$ to L^{OMe} and L^{OEt} ligands resulted in the same product as when using 1 : 1 molar ratio.

1. Mp: 188 °C. Anal. Calcd for $C_{24}H_{22}Cl_2HgN_6O_4$: C, 39.45; H, 3.01; N, 11.51. Found: C, 39.55; H, 3.06; N, 11.58. IR (CsI pellet, cm^{-1}): 3360s, 2960, 1667s, 1600, 1527, 1459s, 1246, 1108, 1020, 910,756. ^1H NMR (CD_3OD, δ from TMS): 9.33(s, 1*H*-pyrazine), 8.83(s, 1*H*-pyrazine), 8.73(s, 1*H*-pyrazine), 8.43(d, 1*H*-phenyl), 7.17–6.97(m, 3*H*-phenyl), 3.97(s, 3*H*–CH_3).

2. Mp: 145 °C. Anal. Calcd for $C_{12}H_{11}Br_2HgN_3O_2$: C, 24.42; H, 1.87; N, 7.12. Found: C, 24.48; H, 1.92; N, 7.17. IR (CsI pellet, cm^{-1}): 3356s, 3072, 1690s, 1598, 1540, 1457s, 1248, 1132, 1022, 908, 752. ^1H NMR (CD_3OD, δ from TMS): 9.35(s, 1*H*-pyrazine), 8.83(s, 1*H*-pyrazine), 8.72(s, 1*H*-yrazine), 8.42(d, 1*H*-phenyl), 7.13–6.98(m, 3*H*-phenyl), 3.97(s, 3*H*–CH_3).

3. Mp: 152 °C. Anal. Calcd for $C_{24}H_{22}Hg_2I_4N_6O_4$: C, 21.06; H, 1.61; N, 6.14. Found: C, 21.12; H, 1.68; N, 6.20. IR (CsI pellet, cm^{-1}): 3360s, 3056, 1686s, 1598, 1542, 1457s, 1250, 1132, 1022, 900,753. ^1H NMR (CD_3OD, δ from TMS): 9.35(s, 1*H*-pyrazine), 8.83(s, 1*H*-pyrazine), 8.73(s, 1*H*-pyrazine), 8.43(d, 1*H*-phenyl), 7.14–6.98(m, 3*H*-phenyl), 3.96(s, 3*H*–CH_3).

4. Mp: 188 °C. Anal. Calcd for $C_{26}H_{26}Cl_2HgN_6O_4$: C, 41.16; H, 3.43; N, 11.08. Found: C, 41.20; H, 3.49; N, 11.13. IR (CsI pellet, cm^{-1}): 3342s, 2980, 1680s, 1600, 1526, 1453s, 1251, 1129, 1042, 901,760. ^1H NMR (CD_3OD, δ from TMS): 9.38(s, 1*H*-pyrazine), 8.85(s, 1*H*-pyrazine), 8.74(s, 1*H*-pyrazine), 8.45(d, 1*H*-phenyl), 7.17–6.98(m, 3*H*-phenyl), 4.21(q, 2*H*–CH_2) and 1.52(t, 3*H*–CH_3).

5. Mp: 145 °C. Anal. Calcd for $C_{13}H_{13}Br_2HgN_3O_2$: C, 25.84; H, 2.15; N, 6.96. Found: C, 25.91; H, 2.19; N, 7.00. IR (CsI pellet, cm^{-1}): 3343s, 2937, 1690s, 1593, 1534, 1452s, 1250, 1129, 1037, 903, 752. ^1H NMR (CD_3OD, δ from TMS): 9.39(s, 1*H*-pyrazine), 8.86(s, 1*H*-pyrazine), 8.76(s, 1*H*-pyrazine), 8.46(d, 1*H*-phenyl), 7.18–7.00(m, 3*H*-phenyl), 4.22(q, 2*H*–CH_2) and 1.52(t, 3*H*–CH_3).

6. Mp: 152 °C. Anal. Calcd for $C_{13}H_{13}HgI_2N_3O_2$: C, 22.36; H, 1.86; N, 6.02. Found: C, 22.41; H, 1.93; N, 6.10. IR (CsI pellet, cm^{-1}): 3340s, 2975, 1686s, 1593, 1535, 1451s, 1249, 1128, 1038, 900,754. ^1H NMR (CD_3OD, δ from TMS): 9.36(s, 1*H*-pyrazine), 8.83(s, 1*H*-pyrazine), 8.72(s, 1*H*-pyrazine), 8.42(d, 1*H*-phenyl), 7.12–6.96(m, 3*H*-phenyl), 4.19(q, 2*H*–CH_2) and 1.49(t, 3*H*–CH_3).

Results and discussion

Synthesis

The ligands L^{OMe} and L^{OEt} were prepared by simply mixing of the same equivalents of *ortho*-anisidine or *ortho*-phenitidine and

Table 1 Structural data and refinement for compounds **1–6**

	1	**2**	**3**
Formula	$C_{24}H_{22}Cl_2HgN_6O_4$	$C_{12}H_{11}Br_2HgN_3O_2$	$C_{24}H_{22}Hg_2I_4\ N_6O_4$
FW	729.97	589.63	1367.26
λ/Å	0.71073	0.71073	0.71073
T/K	120	298	298
Cryst. system	Orthorhombic	Triclinic	Triclinic
Space group	*Pbna*	$P\bar{1}$	$P\bar{1}$
a/Å	6.7123(6)	7.9158(9)	6.9418(11)
b/Å	13.9195(17)	8.1142(8)	7.9241(11)
c/Å	26.783(3)	13.4426(17)	16.6673(19)
α (°)		98.167(9)	82.282(10)
β (°)		94.158(10)	82.029(11)
γ (°)		115.388(8)	66.661(11)
V/Å^3	2502.4(5)	763.49(15)	830.5(2)
D_c/Mg m^{-3}	1.938	2.565	2.734
Z	4	2	1
μ/mm^{-1}	6.409	15.316	12.987
F(000)	1416	540	612
2θ/°	58.58	58.48	58.42
R (int)	0.0990	0.0959	0.0847
GOOF	1.120	1.146	1.149
$R_1{}^a(I > 2\sigma(I))$	0.0616	0.0942	0.0617
w$R_2{}^b(I > 2\sigma(I))$	0.1810	0.1882	0.1521
	4	**5**	**6**
Formula	$C_{26}H_{26}Cl_2HgN_6O_4$	$C_{13}H_{13}Br_2HgN_3O_2$	$C_{13}H_{13}HgI_2N_3O_2$
FW	758.02	603.65	697.65
λ/Å	0.71073	0.71073	0.71073
T/°C	120	298	298
Cryst. system	Monoclinic	Triclinic	Triclinic
Space group	$P2_1/c$	$P\bar{1}$	$P\bar{1}$
a/Å	14.662(3)	7.7934(10)	7.9431(7)
b/Å	28.360(6)	8.7382(12)	8.9284(8)
c/Å	14.515(3)	12.4967(14)	12.9309(12)
α (°)		93.388(10)	93.369(7)
β (°)	114.78(3)	96.104(10)	97.228(7)
γ°		103.975(10)	104.449(7)
V/Å^3	5480.0(2)	817.98(18)	877.10(14)
D_{calc}/Mg.m^{-3}	1.838	2.451	2.642
Z	8	2	2
μ/mm^{-1}	5.857	14.299	12.300
F(000)	2960	559	628
2θ/°	58.48	58.38	58.62
R (int)	0.0667	0.0895	0.1004
GOOF	1.147	1.182	1.098
$R_1{}^a(I > 2\sigma(I))$	0.0535	0.0626	0.0598
w$R_2{}^b(I > 2\sigma(I))$	0.1089	0.1554	0.1602

^{a} $R_1 = \Sigma||F_o| - |F_c||/\Sigma|F_o|$. ^{b} $wR_2 = [\Sigma(w(F_o^2 - F_c^2)^2)/\Sigma w(F_o^2)^2]^{1/2}$.

pyrazinecarboxylic acid in pyridine in the presence of triphenyl phosphite (colorless block crystals, 75% and 85% yield for L^{OMe} and L^{OEt} respectively). Reaction of equimolar amounts of these ligands and HgX_2 (X = Cl, Br and I) in methanol gave the corresponding complexes. Slow evaporation of the solvent resulted in the air-stable colorless needle crystals of **1**, yellow block crystals of **2** and **4–6** and yellow plate crystals of **3**, after a few days.

Structural analysis of 1–3

A simple reaction between HgX_2 and L^{OMe} in methanol afforded well-formed crystals of **1–3**. The asymmetric unit of **1** consists of a half crystallographically independent Hg^{2+} ion, one *N*-(*o*-anisidyl)-2-pyrazinecarboxamide, L^{OMe}, and one chloride ion. As depicted in Fig. 1(a), in this compound, the Hg(II) ion adopts an octahedral (O_h) coordination geometry (maximum deviation of angles fom 90° is ±1.5°) with two N atoms and two O atoms from L^{OMe} ligands and two Cl atoms (Hg–Cl: 2.304(2) Å, Table 2).

The Hg–N and Hg–O distances of 2.812(5) Å and Hg–O 2.922(5) Å, are slightly longer than the other Hg–N and Hg–O distances previously reported but a search on Hg–N/O distances using the Cambridge Structural Database (CSD), resulted in more than 40 and 100 hits which have a longer bond distance than 2.800 Å for Hg–N and 3.000 Å for Hg–O.[20] Coordination geometry around the Hg(II) center in compounds **2** and **3** are square-based pyramid (SBP), Fig. 1(b) and 1(c), respectively, with trigonality indexes (τ)[21] of 0.30 and 0.00 respectively. In both structures of **2** and **3**, the plane of square-based pyramid is occupied by halogen anions (Hg–Br: 2.455(1), 2.472(2) and 3.112(1) Å and Hg–I: 2.611(1), 2.632(1), 3.501(1) and 3.542(1) Å, Table 2). The apical position in both structures is occupied by a

Table 2 Selected bond distances (Å) and angles (°) for complexes **1–6**

	Complex					
Bond distance	**1**	**2**	**3**	**4**	**5**	**6**
Hg–X	2.304(2)	2.455(1)	2.611(1)	2.315(2)	2.413(1)	2.586(1)
		2.472(2)	2.632(1)	2.316(2)		
		3.112(1)[e]	3.501(1)[g]	2.319(2)	2.445(1)	2.608(1)
			3.542(1)[g]	2.312(2)		
Hg–N	2.812(5)	2.447(1)	2.513(7)	2.658(5)	2.538(7)	2.561(7)
				2.760(6)		
				2.723(6)		
				2.713(5)		
Hg–O	2.922(5)[a]	—	—	2.944(6)	—	—
Bond angle						
X–Hg–X	180.0[b]	155.7(1)	160.6(1)	178.3(1)	162.3(1)	160.0(1)
		172.5(1)[e]	160.6(1)[g]			
		93.8(1)[e]	94.5(1)[g]	180.0[i]		
		89.3(1)[e]	94.5(1)[h]			
		93.2(1)[f]	88.5(1)[g]	180.0[j]		
		85.5(1)[f]	88.5(1)[h]			
X–Hg–N	90.6(1) 89.4(1)[b]		101.8(2)	90.7(1)	100.8(2)	100.2(2)
		106..3(3)	97.6(2)	90.8(1)		
				90.2(1)		
		97.9(3)	82.7(2)[g]	89.8(1)		
				91.0(1)	95.9(2)	98.0(2)
		87.1(3)[e]	79.0(2)[h]	87.4(1)		
		88.4(3)[f]		91.9(1)		
				88.1(1)		
Hg–X–Hg	—	90.7(1)[e]	160.5(1)[g]	—	—	—
		86.8(1)[f]	91.5(1)[g]			
			91.2(1)[h]			
X–Hg–O	88.5(1)	—	—	90.3(1)	—	—
	91.5(1)[b]			90.9(1)		
O–Hg–N	90.3(1)[b]	—	—	75.0(1)	—	—
	89.7(1)[c]			118.1(2)		
C=O–Hg	104.1(4)[d]	—	—	118.7(4)	—	—

Symmetry codes:[a] −1 + x, y, z. [b] −x, 1 − y, 2 − z. [c] 1 − x, 1 − y, 2 − z. [d] 1 + x, y, z. [e] −x + 1, −y, −z. [f] 2 − x, −y, −z. [g] −x, 2 − y, −1 − z. [h] 1 − x, 2 − y, −1 − z. [i] −x, 2 − y, −z. [j] 1 − x, 1 − y, −z.

nitrogen atom from the pyrazine ring of the L^{OMe} ligand at a normal distance of 2.447(1) and 2.513(7) Å for **2** and **3** respectively. As is clear from the τ values and geometrical parameters around the central metal atoms, Table 2, in **2**, the Hg(II) has a distorted SBP environment while in **3**, the coordination geometry around Hg(II) is almost perfect SBP.

In **1**, the *o*-anisidyl and pyrazine rings are in-plane with the carbonyl C=O group (the maximum deviation from mean plane through *o*-anisidyl and pyrazine ring is less than 0.125 Å). In this compound, the formation of parallel π–π stacks of the adjacent ligands influences the C=O–Hg angles. The *o*-anisidyl ring involved in the *intramolecular* π–π stacking interaction with the adjacent pyrazine and phenyl rings, is arranged in such a way that the angle between the plane (containing C–CO–N fragment) normal and the O–Hg vector (for geometrical definition see reference 16a), is about 13.85°. In the $\pi_{phen}\cdots\pi_{pyz}$ interactions, the centroid–centroid distance is 3.511 Å. Such π–π interaction effects on the *primary* structure which direct the coordination geometry around Hg(II) containing similar ligands with those discussed in this paper have been reported previously in detail.[16a] Thus, adjacent mercury atoms are linked by C=O–Hg bonds to form a 1D linear polymeric chain spanning along the *a*-axis, Fig. 2(a). The interchain distance of the neighboring mercury atoms bridged by L^{OMe} ligands, is about 6.712 Å. As shown in Fig. 2(b), these 1D linear chains are further linked to each other from one side by head-to-tail dimeric $C–H_{pyz}\cdots Cl–Hg$ and $C=O\cdots H–C_{pyz}$ non-classical hydrogen bonds and from the other side by the weak $C–H...O_{ether}$ intermolecular interactions, Table 3.

Within the asymmetric unit of **2**, each mercury coordinates the a nitrogen donor atom of the pyrazine ring of the L^{OMe} ligand, while each bromine atom in the basal plane bridges two adjacent metal centers to generate a 1D double chain motif in the *a*-direction, Fig. 3(a). In this chain, the Br atom is dicoordinated. The planar organic ligands stack along both sides of the HgBr skeleton and the distance between their mean planes is 7.916 Å, Fig. 3(a).

In **3**, the arrangement of the asymmetric units defines the well-known double-stranded stair motif, Fig. 3(b). In this stair 1D polymer, the translation axis is parallel to the *a*-direction. Although many halide-bridged mercury-based structures have been reported in the literature,[22] but such a stair 1D polymer containing a Hg–I moiety is rare and there is only one reported $[HgI(L)]_n$ stair which contains an imidazolium thiolate ligand.[23] In **3**, the Hg–I bond distances of 3.501(1) and 3.542(1) Å are comparable to that previously reported (3.377 Å) by Popovic *et al.*[23] The iodide anion in the stair is tricoordinated in a highly distorted pyramidal geometry (diagonal $I\cdots I^{iii}$ = 4.369 Å). The organic ligand moieties approximately preserve their planarity and stack along both sides of the HgI skeleton; the distance between their main planes being 6.942 Å, Fig. 3(b). This 1D double chain in **2** and double-stranded stair chain in **3**, are

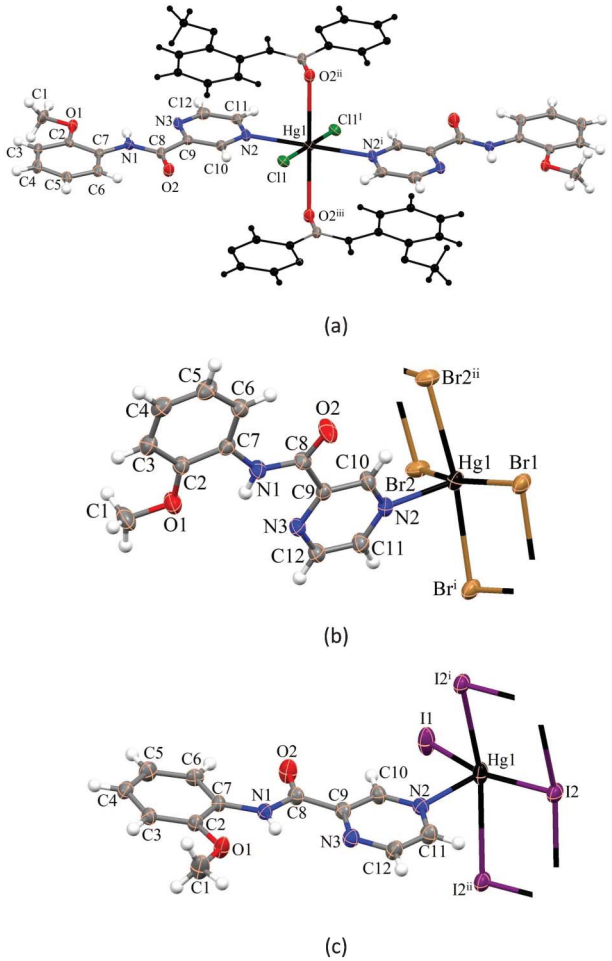

Fig. 1 Portion of the structure of coordination polymers formed between L^{OMe} and $HgCl_2$, **1**, (a), $HgBr_2$, **2**, (b), and HgI_2, **3**, (c), showing coordination geometry around central metal. Symmetry codes; (a) i) −x, 1 − y, 2 − z, ii)−1 + x, y, z, iii) 1 − x, 1 − y, 2 − z, (b) i) 2 − x, −y, −z, ii) 1 − x, −y, −z and (c) i) −x, 2 − y, −1 − z, ii) 1 − x, 2 − y, 1 − z.

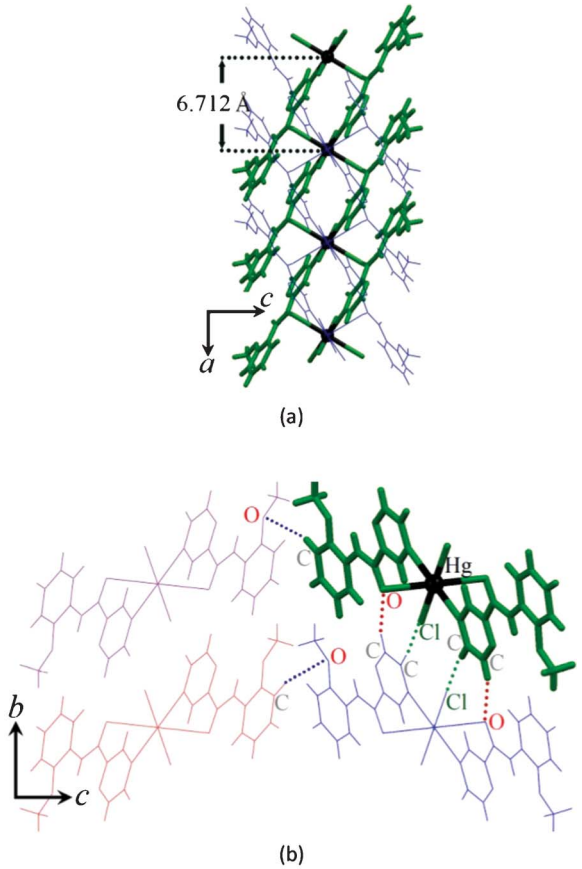

Fig. 2 Representation of 1D linear polymeric chain in **1** viewed down [010], (a), and a side view representation of **1** in *a*-direction showing the association of the adjacent molecules in the chain, through an additional head-to-tail dimeric C–H_{pyz}···Cl–Hg and C=O···H–C_{pyz} non-classical hydrogen bonds and C–H···O_{ether} intermolecular interactions, (b). Different colours show different adjacent linear chains.

further linked to adjacent chains from one side by head-to-tail dimeric C–H_{phen}···O=C and C–H_{methyl}···O_{ether} non-classical hydrogen bonds in **2** and **3**, respectively, and from the other side by the intermolecular C–H_{pyz}···Br–Hg and C–H_{phen}···I–Hg interactions, respectively, Fig. 4(a) and 4(b), Table 3.

Planar organic ligand moieties along both sides of the HgX skeleton in adjacent chains are liked by C=O···π_{phen} interactions with C(carbonyl)–centroid(phen) distances of 3.651 and 3.581 Å for **2** and **3** respectively, Table 3, Fig. 4(c) and 4(d). It is notable that in **2**, π_{pyz}···π_{phen} (with centroid–centroid distance of 3.696 Å) cooperates with this C=O···π_{phen} interactions in the stabilization of the packing, Fig. 4(c), Table 3.

Structural analysis of 4–6

Compound **4** consists of two different three-nuclear, part 4A, and mono-nuclear, part 4B, mercury complexes. This compound displays 2/*m* point symmetry in the solid state, making half of the three-nuclear and mono-nuclear part of this compound crystallographically unique. Thus, in **4**, each asymmetric unit consists of 2.5 crystallographically independent Hg(II) centers, four chloride ions, and three neutral L^{OEt} ligands, Fig. 5(a). Therefore, for this complex, Table 2 shows three sets of values. In part 4A, Hg1 is in a slightly distorted square-based pyramidal geometry (SBP), with trigonality index (τ) of 0.19, coordinated by two L^{OEt} ligands and two Cl atoms in the basal plane and in *cis* position and one carbonyl oxygen atom of the third L^{OEt} ligand at the vertex. The recent L^{OEt} ligand, acts as an angular bridge *via* carbonyl oxygen and pyrazine nitrogen atoms to link Hg1 and Hg2 ions, meanwhile, the Hg2 atom, in a square-planar geometry, is also bonded to two Cl atoms in the *cis* position and to another bridged L^{OEt} ligand between Hg2 and $Hg1^{i}$ (symmetry code: −x, 2 − y, −z), to form a three-nuclear complex. Part 4B complex, features slightly distorted square-planar (SP) geometry. The Cl–Hg–Cl and N–Hg–N axis are constrained to linearity by crystallographic symmetry, Table 2. The angles of Cl–Hg–N range from 88.1(1) to 91.9(1)°. It is notable that there is a very weak Hg···O interaction between the Hg3 atom and the two adjacent carbonyl oxygen atoms ($Hg3\cdots O3^{iii}$ = 3.206 Å, symmetry code: (iii) 1 − x, −½ + y, ½ − z) in the part 4B coordination center.

In isostructural compounds **5** and **6** the mercury atom is located in a three coordination environment, Fig. 5(b) and 5(c), chelating with two halogen atoms and one pyrazine nitrogen atom from ligand L^{OEt} with bond lengths of Hg–X = 2.413(1)

Table 3 Significant intermolecular interactions (interatomic distance (Å) and bond angles (°)) found in the structures of **1–6**

D–H···A	D–H	H···A	D···A	D–H···A
compound **1**				
$C11_{pyz}$–H11···Cl1–Hg[a]	0.930	2.864	3.793(12)	177
$C12_{pyz}$–H12···O2=C[b]	0.930	2.421	3.282(9)	154
$C3_{phen}$–H3···O_{ether}[c]	0.970	2.740	3.688(7)	165
compound **2**				
$C12_{pyz}$–H12···Br2–Hg[d]	0.930	3.031	3.716(11)	132
$C6_{phen}$–H6···O2=C[e]	0.930	2.639	3.507(12)	156
Cg(π_{phen})···C8=O[f]	—	—	3.651	—
Cg(π_{pyz})···Cg(π_{phen})[g]	—	—	3.696	—
compound **3**				
$C4_{pyz}$–H4···I1–Hg[h]	0.930	3.037	3.800(10)	140
$C1_{methyl}$–H1C···$O1_{ether}$[i]	0.960	2.550	3.452(13)	156
Cg(π_{phen})···C8=O[j]	—	—	3.581	—
compound **4**				
$C51_{methyl}$–H51A···Cl2–Hg[k]	0.970	2.740	3.688(7)	165
$C7_{phen}$–H7···O1=C	0.930	2.320	2.917(8)	121
$C10_{phen}$–H10···O3=C[l]	0.930	2.520	3.204(8)	131
$C20_{phen}$–H20···O3=C	0.930	2.360	2.937(8)	120
$C23_{phen}$–H23···O1=C[m]	0.930	2.420	3.157(8)	136
$C33_{phen}$–H33···O5=C	0.930	2.350	2.935(8)	121
$C36_{phen}$–H36···O7=C[n]	0.930	2.500	3.222(8)	134
$C46_{phen}$–H46···O7=C	0.930	2.320	2.910(9)	121
$C49_{phen}$–H49···O5=C[o]	0.930	2.460	3.145(8)	130
C_{methyl}–H52B···Cg(π_{phen})[p]	—	—	2.854(7)	—
C_{methyl}–H13A···Cg(π_{phen})[q]	—	—	2.846(7)	—
Cg(π_{phen})···Cg(π_{pyz})[q]	—	—	3.597(3)	—
Cg(π_{phen})···Cg(π_{pyz})[q]	—	—	3.606(4)	—
Cg(π_{phen})···Cg(π_{pyz})[r]	—	—	3.791(4)	—
compound **5**				
$C13_{methyl}$–H13C···O1=C[s]	0.960	2.430	3.373(14)	169
Cg(π_{pyz})···Cg(π_{phen})[t]	—	—	3.710	—
Hg1···Cg(π_{phen})[t]	—	—	3.501	—
compound **6**				
$C13_{methyl}$–H13C···O1=C[u]	0.960	2.560	3.501(15)	168
Cg(π_{pyz})···Cg(π_{phen})[v]	—	—	3.790	—
Hg1···Cg(π_{phen})[w]	—	—	3.540	—

Symmetry codes:[a] −x, ½ + y, z. [b] 1 − x, 1/2 + y, z. [c] 1/2 + x, y, 3/2 − z. [d] 2 − x, 1 − y, −z. [e] 1 − x, −y, 1 − z. [f] 1 − x, 1 − y, 1 − z. [g] 2 − x, 1 − y, 1 − z. [h] 1 − x, 1 − y, −z. [i] −x, 3 − y, −z. [j] 1 − x, 2 − y, −z. [k] 1 + x, y, z. [l] −x, −½ + y, ½ − z. [m] 1 − x, ½ + y, ½ − z. [n] x, 3/2 − y, ½ + z. [o] 1 + x, 3/2 − y, −½ + z. [p] −1 + x, 3/2 − y, −1/2 + z. [q] −1 + x, y, z. [r] −x, ½ + y, ½ − z. [s] −1 + x, −1 + y, z. [t] −x, 1 − y, 1 − z. [u] 1 + x, 1 + y, z. [v] 2 − x, 2 − y, 1 − z. [w] 1 − x, 2 − y, 1 − z.

and 2.445(1) Å for **5** and 2.586(1) and 2.608(1) Å for **6** and Hg–N = 2.538(7) and 2.561(7) for **5** and **6** respectively, Table 2. The X–Hg–X angle of 162.3(1) and 160.0(1)° for **5** and **6**, respectively, shows that the geometry around the metal center is slightly distorted T-shape.

As shown in Fig. 6, in **4**, monomeric and trimeric molecules are linked to adjacent molecules by $\pi_{phen}\cdots\pi_{pyz}$, C–$H_{methyl}\cdots$Cl–Hg, C–$H_{methyl}\cdots\pi_{phen}$ interactions, Table 3. As depicted in Fig. 6, these intermolecular interactions act as cooperative factors with several C–$H_{methyl}\cdots$O=C interactions to generate three dimensional packing.

The non-classical hydrogen bonds in **5** and **6**, which are those between C–H_{methyl} donor and carbonyl oxygen acceptor, form a one dimensional chain, Fig. 7(a) and 7(b), respectively. These 1D chains are further linked by Hg···π and head-to-tail dimeric $\pi_{phen}\cdots\pi_{pyz}$ interactions in the other direction, Table 3. For the $\pi_{phen}\cdots\pi_{pyz}$ interactions, the centroid–centroid distance and for the Hg···π, the metal–centroid distance is about 3.710 and 3.501 Å, for **5** and 3.790 and 3.540 Å for **6**, respectively.

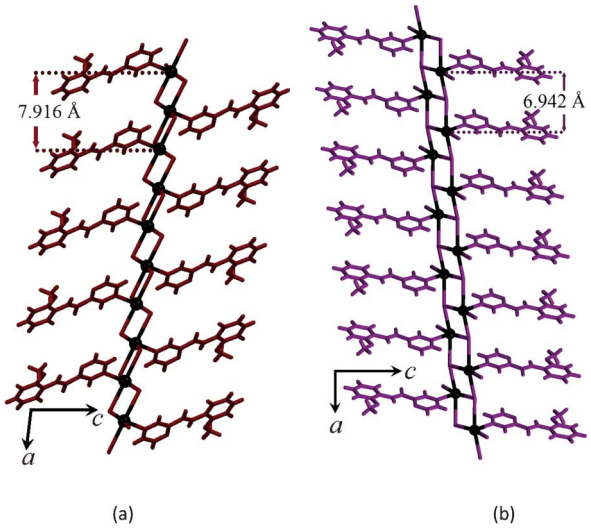

Fig. 3 Representation of a 1D double chain in **2**, (a), and stair 1D polymer in **3**, (b), in *b*-direction.

Influence of ligand substituent on molecular architecture

Understanding and controlling the structural assemblies in the solid state requires investigations on families of materials which have been designed in such a way as to systematically delineated the effects of different factors on the resultant supramolecular and structural properties.

In this regard, the effect of the ligand substituent and the effect of different halogen anions, on the coordination geometry and three-dimensional supramolecular architecture of the six coordination compound of mercury(II) has been studied. In the following discussion, we will focus on similarities and differences between the various coordination compounds.

Much of the difference in structural motifs can be explained by the changing of the steric environment of the ligands, but the role of the different halogen anions should not be neglected. In the first series, in compounds **1–3** where the carboxamide ligand is similar, our results clearly show that the coordinated anion has a remarkable effect on the coordination geometry as well as the structural motif of the resulting one-dimensional polymers. The coordination geometry around the Hg(II) center in compound **1** adopts an O_h coordination geometry. The situation for compounds **2** and **3** (where X is Br and I anions respectively), is quite different from that of compound **1**, both in the coordination geometry of the Hg(II) centers and in the kind of 1D polymeric structures. By replacing coordinated anions from chloride to bromide or iodide, the coordination geometry changed from O_h to SBP. It is notable, that although the structural motif in compounds **1–3** are different, the structural analysis show that in all three structures, 1D coordination polymers have resulted, Table 4.

It is interesting to compare the coordination core and structural assembly of the present complexes with respect to the growing steric bulk of the aryl group on the phenyl ring. When compared to the L^{OMe} substituent, the steric properties of the L^{OEt} group significantly alter the molecular architecture and coordination sphere of complexes containing *N*-(aryl)-2-pyrazinecarboxamide ligand. For the $HgCl_2$ adduct, from **1** to **4**, the

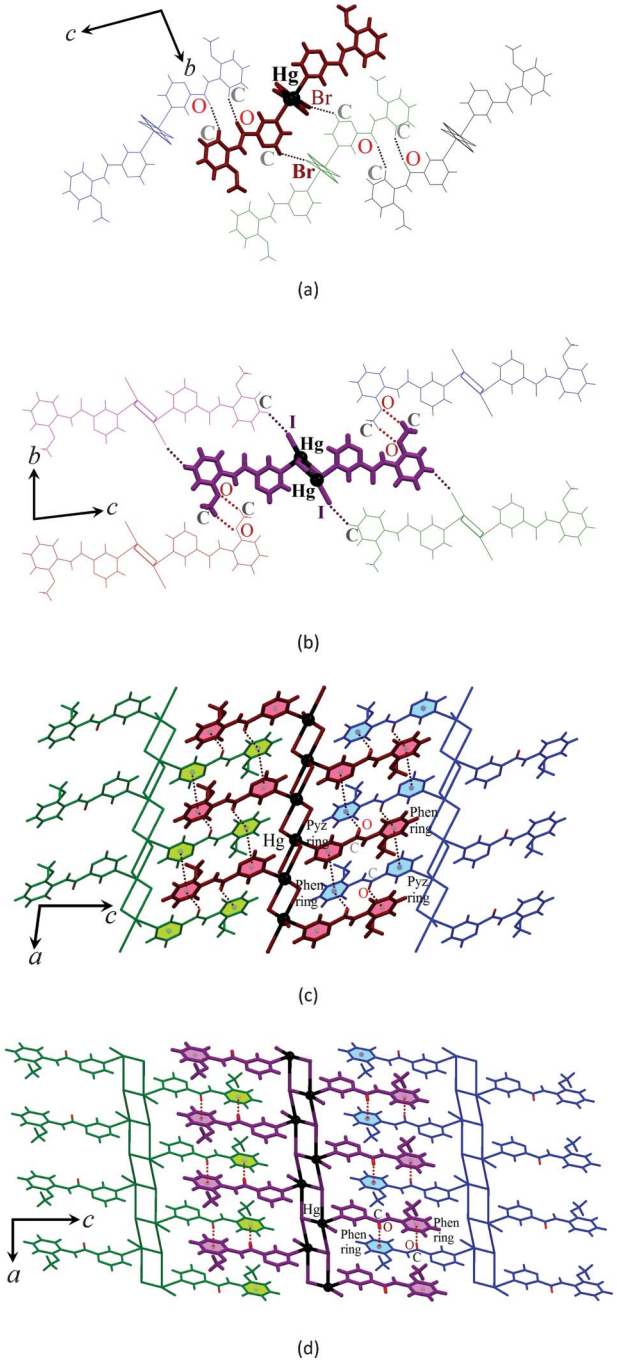

Fig. 4 A side view representation of **2**, (a), and **3**, (b), in *a*-direction showing the association of the adjacent molecules in the chains, through head-to-tail dimeric C–H_{phen}···O=C and C–H_{pyz}···Br–Hg in **2** and head-to-tail dimeric C–H_{methyl}···O_{ether} and C–H_{phen}···I–Hg non-classical hydrogen bonds in **3**. Different colours show different adjacent linear chains. A representation of part of **2** and **3** showing the cooperation of C=O···π_{phen} and π_{pyz}···π_{phen} interactions in **2**, (c), and C=O···π_{phen} interactions in **3**, (d), in generation of three dimensional packing.

coordination sphere changes from O_h to SBP-SP. For HgX_2 adducts (while X = Br and I), the coordination geometry around the central atom has been changed from SBP for **2** and **3** to T-shape for **5** and **6**. As listed in Table 4, for the second series, compounds **4–6** have non-polymeric structures. In **4** the trimeric/monomeric motif resulted while in isostructural **5** and **6**

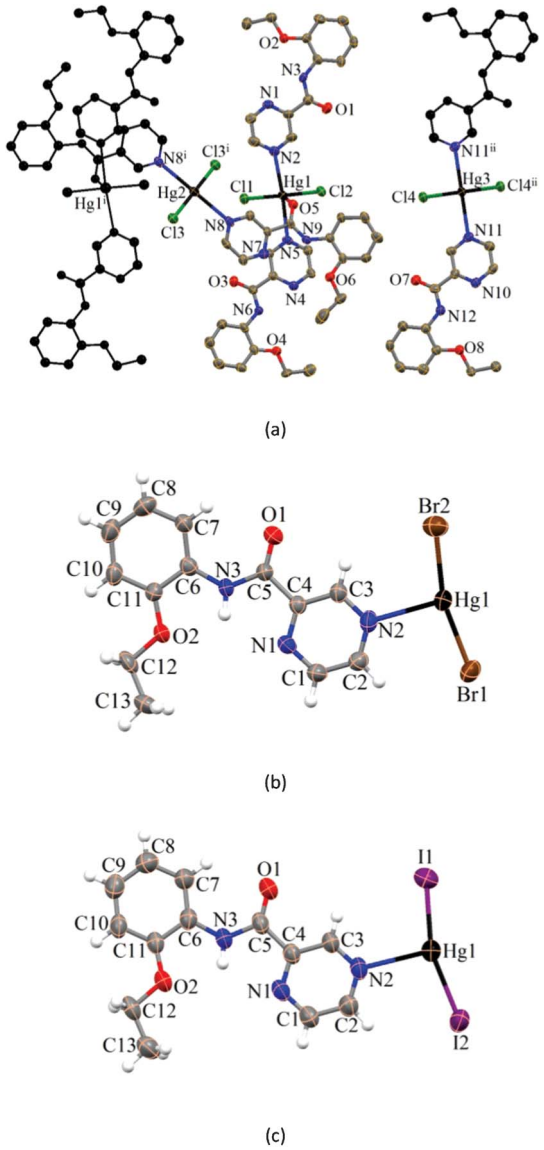

Fig. 5 Structure of coordination compound formed between L^{OEt} and $HgCl_2$, **4**, (a), $HgBr_2$, **5**, (b), and HgI_2, **6**, (c), showing coordination geometry around the central metal. Symmetry codes; i) −x, 2 − y, −z, ii) 1 − x, 1 − y, −z.

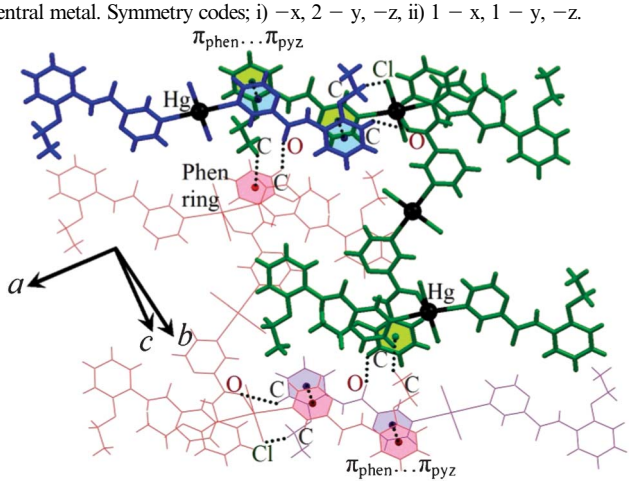

Fig. 6 A side view representation of **4** showing the cooperation of π_{phen}···π_{pyz}, C–H_{methyl}···Cl–Hg, C–H_{methyl}···π_{phen} and C-H_{methyl}···O=C interactions in generation of three dimensional packing.

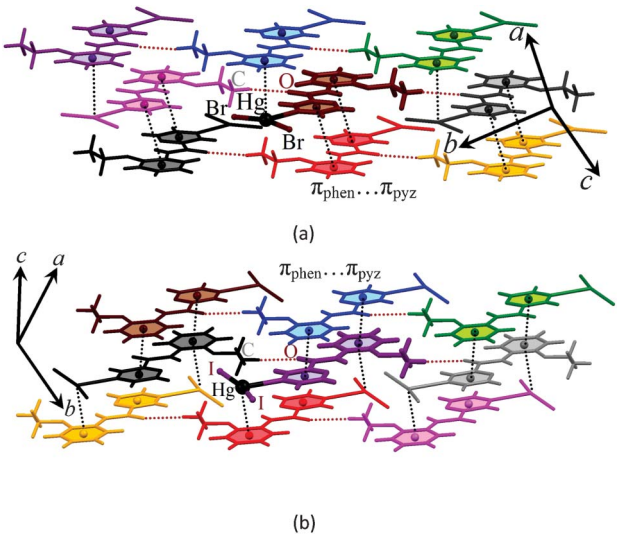

Fig. 7 A representation of part of the unit cell contents of **5**, (a) and **6**, (b), showing the non-classical C–$H_{methyl}\cdots$O=C hydrogen bonds, Hg$\cdots\pi$ and head-to-tail dimeric $\pi_{phen}\cdots\pi_{pyz}$ interactions.

compounds, discrete three coordinated mercury compounds were formed.

These later three structures, together with the HgX_2 adduct with L^{OEt}, clearly add further evidence that even in the case of simple and monodentate ligands such as *N*-(aryl)-pyrazinecarboxamide, the substituents on the organic ligand can influence the structural motif by its steric properties. It is proper to consider why such a drastic substituent effect is induced. The most significant feature is the similar electronic properties of the ligands chosen for this study, with respect to the donating pyrazine nitrogen atom. The same pyrazine–CONH–aryl moiety is presented in the two ligands. The small angle between the pyrazine–phenyl main planes (less than 8.46°), shows the coplanarity of the ligands in all six compounds. In spite of this similarity and molecular rigidity, the difference in the steric properties of the ligands is quite remarkable in the changes of structural assemblies and coordination geometries from L^{OMe} to L^{OEt}. The difference in structural motifs can thus be explained by the changing of the steric properties of the ligands. The role of the size and nature of the halogen anions can also affect the nature of the mercury coordination sphere. Based on these results, we tentatively propose that the most important factors dictating polymeric or non-polymeric structures are the steric properties of the ligands surrounding the mercury atom. These steric properties affects the nature of the intermolecular interactions in these complexes and therefore indirectly affect the structural assemblies and coordination geometries indirectly.

The crystal packing patterns of **1–3** were analyzed in terms of C=O$\cdots\pi$ and $\pi\cdots\pi$ in some cases and non-classical weak intermolecular interactions such as C–H$\cdots$O and C–H$\cdots$X–Hg (X = halogen) in all three compounds. The analysis shows that the changing of the steric profile of the ligands from *o*-anisidyl to *o*-phenitidyl, successfully changed some of the synthons seen in the **1–3** packings and that the new compounds, specially compounds **5** and **6** adopt other packing strategies, based on Hg$\cdots\pi$ contacts.

Conclusion

We have shown that by varying the steric profile of *N*-(aryl)-2-pyrazinecarboxamide ligands, the nature of the structural assemblies and coordination geometries of mercury coordination polymers can be tuned. Structural analysis of mercury(II) halides containing the *N*-(*o*-anisidyl)-2-pyrazinecarboxamide ligand demonstrated that the assembly process produced an infinite 1D linear chain, 1D double chain and 1D ladder chain in chloride, bromide and iodide adducts respectively. When compared to the *o*-anisidyl substituent, the steric properties of the *N*-(*o*-phenitidyl)-2-pyrazinecarboxamide ligand significantly alter the molecular architecture and coordination sphere of the complexes. For the $HgCl_2$ adduct, the coordination sphere changes from O_h to square-based pyramid/square-planar (SBP/SP). For the HgX_2 adducts (while X = Br and I), the coordination geometry around the central atom has been changed from SBP to T-shape. For the second series, discrete

Table 4 Coordination geometries and list of intermolecular interactions controlling the packing of polymeric and non-polymeric compounds **1–6**

Complex	Coordination geometry	Main factors controlling the packing	Polymeric/non-polymeric
1, $[HgCl_2(L^{OMe})_2]_n$	O_h	C–$H_{pyz}\cdots$Cl–Hg C–$H_{phen}\cdots O_{ether}$ C=O$\cdots$H–C_{pyz}	1D linear chain
2, $[HgBr_2(L^{OMe})]_n$	SBP	C–$H_{pyz}\cdots$Br–Hg C–$H_{phen}\cdots$O=C C=O$\cdots\pi_{phen}$ $\pi_{pyz}\cdots\pi_{phen}$	1D double chain
3, $[Hg_2I_4(L^{OMe})]_n$	SBP	C–$H_{phen}\cdots$I–Hg C–$H_{methyl}\cdots O_{ether}$ C=O$\cdots\pi_{phen}$	1D ladder chain
4, $[Hg_3Cl_6(L^{OEt})_3]\cdot[HgCl_2(L^{OEt})]$	SBP-SP-SBP/SP	C–$H_{methylene}\cdots$Cl–Hg C–$H_{phen}\cdots$O=C $\pi_{phen}\cdots\pi_{pyz}$ C–$H_{methyl}\cdots\pi_{phen}$	Trimmer/Monomer
5, $[HgBr_2(L^{OEt})]$	T-shape	Hg$\cdots\pi_{phen}$ C–$H_{methyl}\cdots$O=C $\pi_{pyz}\cdots\pi_{phen}$	Monomer
6, $[HgI_2(L^{OEt})]$	T-shape	Hg$\cdots\pi_{phen}$ $\pi_{pyz}\cdots\pi_{phen}$ C–$H_{methyl}\cdots$O=C	Monomer

non-polymeric coordination compounds have been formed. While substituents on the terminal phenyl rings do not influence the planarity of the *N*-(aryl)-2-pyrazinecarboxamide, they do significantly influence the intermolecular stacking arrangements for these compounds in the solid state. A combination of several weak and medium intermolecular interactions, including C=O···π, π···π, C–H···O, Hg···π and C–H···X–Hg (X = halogen) interactions determine the structural assemblies and coordination geometries in these compounds.

Acknowledgements

We would like to thank the Graduate Study Councils of Shahid Beheshti University, General Campus and the Iran National Science Foundation (grant No. 87041984) for financial support.

References

1 (*a*) E. R. T. Tiekink and J. J. Vital Frontiers, in *Crystal Engineering*, John Wiley & Sons: Chichester, U.K., 2006; (*b*) F. Grepioni and D. Braga, *Making Crystals by Design-From Molecules to Molecular Materials, Methods, Techniques, Applications*, Wiley-VCH: Weinheim, Germany, 2007; (*c*) G. R. Desiraju, *The Crystal as a Supramolecular Entity*, John Wiley & Sons: New York, 1996; (*d*) J. –M. Lehn, *Supramolecular Chemistry: Concepts and Prespectives*, Wiley-VCH: Weinheim, Germany, 1995; (*e*) G. R. Desiraju, *Crystal Engineering; The Design of Organic Solids*, Elsevier: Amsterdam, 1989; (*f*) J. W. Steed and J. L. Atwood, *Supramolecular Chemistry*, Wiley: Chichester, 2000; (*g*) L. Brammer, *Chem. Soc. Rev.*, 2004, **33**, 476; (*h*) D. Braga, L. Brammer and N. R. Champness, *CrystEngComm*, 2005, **7**, 1; (*i*) G. R. Desiraju, *Angew. Chem., Int. Ed.*, 2007, **46**, 8342; (*j*) A. Nangia and G. R. Desiraju, *Acta Crystallogr., Sect. A: Found. Crystallogr.*, 1998, **54**, 934; (*k*) G. Férey, *Chem. Soc. Rev.*, 2008, **37**, 191; (*l*) C. B. Aakeröy, N. R. Champness and C. Janiak, *CrystEngComm*, 2010, **12**, 22.

2 (*a*) L. Ma and W. Lin, *J. Am. Chem. Soc.*, 2008, **130**, 13834–13835; (*b*) R. Peng, S. -R. Deng, M. Li, D. Li and Z.-Y. Li, *CrystEngComm*, 2008, **10**, 590–597; (*c*) I. S. Lee, D. M. Shin and Y. K. Chung, *Chem.–Eur. J.*, 2004, **10**, 3158–3165; (*d*) X. -C. Huang, D. Li and X.-M. Chen, *CrystEngComm*, 2006, **8**, 351–355; (*e*) P. A. Gale, M. E. Light and R. Quesada, *Chem. Commun.*, 2005, 5864–5866.

3 (*a*) P. Mahata, M. Prabu and S. Natarajan, *Cryst. Growth Des.*, 2009, **9**, 3683–3691; (*b*) J. -P. Zhao, B.-W. Hu, Q. Yang, T.-L. Hu and X.-H. Bu, *Inorg. Chem.*, 2009, **48**, 7111–7116.

4 (*a*) J. S. Seo, D. Whang, H. Lee, S. I. Jun, J. Oh, Y. J. Jeon and K. Kim, *Nature*, 2000, **404**, 982–986; (*b*) L. Pan, H. Liu, X. X. Lei, D. H. Huang, N. J. Olsen and J. Li Turro, *Angew. Chem., Int. Ed.*, 2003, **42**, 542–546.

5 (*a*) H. R. Khavasi and B. Mir Mohammad Sadegh, *Inorg. Chem.*, 2009, **48**, 5593; (*b*) X. -S. Wang, S. Ma, P. M. Forster, D. Yuan, J. Eckert, J. J. Lpez, B. J. Murphy, J. B. Praise and H.-C. Zhou, *Angew. Chem., Int. Ed.*, 2008, **47**, 7263–7266; (*c*) S. Mosaoka, D. Tanaka, Y. Nakanishi and S. Kitagawa, *Angew. Chem., Int. Ed.*, 2004, **43**, 2530–2534.

6 (*a*) F. Yu, X. -J. Kong, Y.-Y. Zheng, Y. P. Ren, L.-S. Long, R. B. Huang and L.-S. Zheng, *Dalton Trans.*, 2009, 9503–9509; (*b*) S. T. Wu, L. S. Long, R. B. Huang and L. S. Zheng, *Cryst. Growth Des.*, 2007, **7**, 1746–1752; (*c*) X. L. Wang, C. Qin, E. B. Wang, Y. G. Li, Z. M. Su, L. Xu and L. Carlucci, *Angew. Chem., Int. Ed.*, 2005, **44**, 5824–5827.

7 (*a*) X. Zhang, X. -P. Zhou and D. Li, *Cryst. Growth Des.*, 2006, **6**, 1440–1444; (*b*) Y. -P. Ren, X.-J. Kong, L.-S. Long, R.-B. Huang and L.-S. Zheng, *Cryst. Growth Des.*, 2006, **6**, 572–576.

8 (*a*) Y. Guo, W. Dou, X. Zhou, W. Liu, W. Qin, Z. Zang, H. Zhang and D. Wang, *Inorg. Chem.*, 2009, **48**, 3581–3590; (*b*) G. -X. Liu, K. Zhu, H. Chen, R.-Y. Huang and X.-M. Ren, *CrystEngComm*, 2008, **10**, 1527–1530; (*c*) Y. T. Wang, H. H. Fan, H. Z. Wang and X. M. Chen, *Inorg. Chem.*, 2005, **44**, 4148–4150; (*d*) C. N. R. Rao, S. Natarajan and R. Vaidhyanathan, *Angew. Chem., Int. Ed.*, 2004, **43**, 1466–1496; (*e*) M. Eddaoudi, J. Kim, D. Vodak, A. Sudik, J. Wachter, M. O'Keefe and O. M. Yaghi, *Proc. Natl. Acad. Sci. U. S. A.*, 2002, **99**, 4900–4904; (*f*) M. R. Bermejo, R. Pedrido, A. M. González-Noya, M. J. Romero, M. Vázquez and L. Sorace, *New J. Chem.*, 2003, **27**, 1753–1759.

9 (*a*) L. Carlucci, G. Ciani, D. M. Proserpio and S. Rizzato, *New J. Chem.*, 2003, **27**, 483–489; (*b*) T. Burchell and R. J. Puddaphatt, *Inorg. Chem.*, 2005, **44**, 3718–3730; (*c*) A. Rodríguez-Diéguez, A. J. Mota, J. M. Seco, M. A. Palacios, A. Romerosa and E. Colacio, *Dalton Trans.*, 2009, 9578–9586.

10 (*a*) C. S. Lai, Y. X. Lian, T. C. Yap and E. R. T. Tiekink, *CrystEngComm*, 2002, **4**, 596–600; (*b*) E. R. T. Tiekink, *CrystEngComm*, 2003, **5**, 101–113; (*c*) C. S. Lai, S. Liu and E. R. T. Tiekink, *CrystEngComm*, 2004, **6**, 221–226; (*d*) C. S. Lai and E. R. T. Tiekink, *CrystEngComm*, 2004, **6**, 593–605; (*e*) D. Chen, C. S. Lai and E. R. T. Tiekink, *CrystEngComm*, 2006, **8**, 51–58; (*f*) E. R. T. Tiekink, *CrystEngComm*, 2006, **8**, 104–118; (*g*) R. E. Benson, C. A. Ellis, C. E. Lewis and E. R. T. Tiekink, *CrystEngComm*, 2007, **9**, 930–941; (*h*) J.-G. Kang, J.-S. Shin, D.-H. Cho, Y.-K. Jeong, C. Park, S. F. Soh, C. S. Lai and E. R. T. Tiekink, *Cryst. Growth Des.*, 2010, **10**, 1247–1256.

11 S.-L. Li, Y.-Q. Lan, J.-C. Ma, J.-F. Ma and Z.-M. Su, *Cryst. Growth Des.*, 2010, **10**, 1161–1170.

12 R. Mondal, M. K. Bhunia and K. Dhara, *CrystEngComm*, 2008, **10**, 1167–1174.

13 (*a*) D. B. Grotjahn, S. Van, D. Combs, D. A. Lev, C. Schneider, C. D. Incarvito, K.-C. Lam, G. Rossi, A. L. Rheingold, M. Rideout, C. Meyer, G. Hernandez and C. Mejorado, *Inorg. Chem.*, 2003, **42**, 3347–3355; (*b*) S. K. Nayak, K. N. Venugopala, D. Chopra, Vasu and T. N. Guru Row, *CrystEngComm*, 2010, **12**, 1205–1216.

14 (*a*) W. Niu, M. D. Smith and J. J. Lavigne, *Cryst. Growth Des.*, 2006, **6**, 1274–1277; (*b*) S. Varughese and S. M. Draper, *Cryst. Growth Des.*, 2010, **10**, 2571–2580.

15 (*a*) Y. Habata, K. Noto and F. Osaka, *Inorg. Chem.*, 2007, **46**, 6529–6534; (*b*) L. Zhou, Y. Wang, C. Zhou, C. Wang, Q. Shi and S. Peng, *Cryst. Growth Des.*, 2007, **7**, 300–306.

16 (*a*) H. R. Khavasi and M. Azizpoor Fard, *Cryst. Growth Des.*, 2010, **10**, 1892; (*b*) H. R. Khavasi, A. R. Salimi, H. Eshtiagh-Hosseini and M. M. Amini, *CrystEngComm*, 2011, **13**, 3710–3717.

17 S. M. S. V. Wardell, M. V. N. de Souza, T. R. A. Vasconcelos, M. L. Ferreira, J. L. Wardell, J. N. Low and C. Glidewell, *Acta Crystallogr., Sect. B: Struct. Sci.*, 2008, **64**, 84–100.

18 (*a*) *X–AREA: Program for the Acquisition and Analysis of Data*, version 1.30; Stoe & Cie GmbH, Darmstadt, Germany, 2005; (*b*) *X–RED: Program for Data Reduction and Absorption Correction*, version 1.28b, Stoe & Cie GmbH, Darmstadt, Germany, 2005; (*c*) *X–SHAPE: Program for crystal optimization for numerical absorption correction*, version 2.05, Stoe & Cie GmbH, Darmstadt, Germany, 2004; (*d*) G. M. Sheldrick, *SHELX97: Program for Crystal Structure Solution and Refinement*, University of Göttingen, Göttingen, Germany, 1997; (*e*) *X-STEP32: Crystallographic Package*, Version 1.07b, Stoe & Cie GmbH, Darmstadt, Germany, 2000.

19 K. Sasan, H. R. Khavasi and M. D. Davari, *Monatsh. Chem.*, 2008, **139**, 773–780.

20 Cambridge Structural Database, version 5.33, November 2011, Cambridge, UK.

21 A.W. Addison, T.N. Rao, J. Reedijk, J. Van Rijn, G.C. Verschoor and J. Che, *J. Chem. Soc., Dalton Trans.*, 1984, 1349–1356.

22 For example see: (*a*) S. Y. Lee, S. Park, H. J. Kim, J. H. Jung and S. S. Lee, *Inorg. Chem.*, 2008, **47**, 1913; (*b*) T. J. Burchell and R. Puddephatt, *Inorg. Chem.*, 2005, **44**, 3718; (*c*) C. P. McArdle, S. Van, M. C. Jennings and R. J. Puddephatt, *J. Am. Chem. Soc.*, 2002, **124**, 3959; (*d*) M. -C. Brandys and R. J. Puddephatt, *J. Am. Chem. Soc.*, 2002, **124**, 3946; (*e*) W. J. Hunks, M. C. Jennings and R. Puddephatt, *Inorg. Chem.*, 2000, **39**, 2699; (*f*) C.-Y. Su, A. M. Goforth, M. D. Smith and H.-C. zur Loye, *Inorg. Chem.*, 2003, **42**, 5685; (*g*) D. Gudat, M. Nieger and M. Schrott, *Inorg. Chem.*, 1997, **36**, 1476; (*h*) M. Tschinkl, A. Schier, J. Riede and F. P. Gabbai, *Angew. Chem., Int. Ed.*, 1999, **38**, 3547; (*i*) M. S. Bharara, T. H. Bui, S. Parkin and D. A. Atwood, *Inorg. Chem.*, 2005, **44**, 5753; (*j*) X.-F. Wang, Y. Lv, T.-A. Okamura, H. Kawaguchi, G. Wu, W.-Y. Sun and N. Ueyama, *Cryst. Growth Des.*, 2007, **7**, 1125; (*k*) N. D. Draper, R. J. Batchelor and D. B. Leznoff, *Cryst. Growth Des.*, 2004, **4**, 621; (*l*) D. J. Eisler and R. J. Puddephatt, *Cryst. Growth Des.*, 2005, **5**, 57; (*m*) S. R. Batten, A. R. Harris, K. S. Murray and J. P. Smith, *Cryst. Growth Des.*, 2002, **2**, 87.

23 Z. Popovic, Z. Soldin, D. Matkovic-Calogovic, G. Pavlovic, M. Rajic and G. Giester, *Eur. J. Inorg. Chem.*, 2002, 171.